



Influence of view factors on intra-urban air temperature and thermal comfort variability in a temperate city

Hai Yan ^{a,*}, Fan Wu ^b, Xinge Nan ^a, Qian Han ^a, Feng Shao ^a, Zhiyi Bao ^a

^a College of Landscape Architecture, Zhejiang A & F University, Hangzhou 311300, China

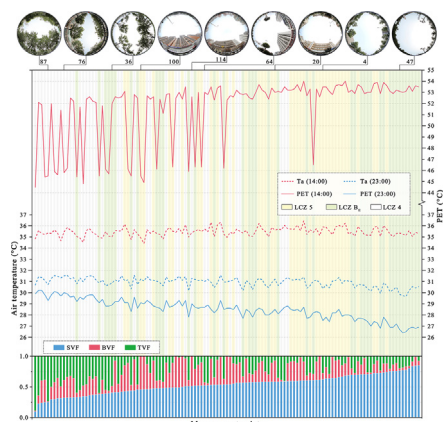
^b School of Civil Engineering and Architecture, Zhejiang Sci-Tech University, Hangzhou 310018, China



HIGHLIGHTS

- Urban thermal environment is greatly influenced by urban geometry.
- SVF has a warming effect during daytime, but the opposite effect at night.
- BVF is a key parameter in determining nighttime urban air temperature.
- Increasing TVF could be one effective way to improve urban outdoor thermal environment.

GRAPHICAL ABSTRACT



ARTICLE INFO

Editor: Pavlos Kassomenos

Keywords:

Urban geometry
View factor
Air temperature
Thermal comfort
Temperate climate

ABSTRACT

Urban geometry is known to be one of the major factors in explaining the intra-urban temperature variations. A commonly used indicator to describe the urban geometry is the sky view factor. However, the existing studies have shown that the relationship between SVF and urban temperature is quite contradictory. This suggests that a single SVF cannot accurately quantify the urban geometry. For comparison, we here propose to use view factors, including sky, building and tree view factors (SVF, BVF, and TVF, respectively), to accurately quantify the three-dimensional urban geometry. Based on microclimate measurements conducted in Beijing Olympic Park and its surrounding urban environment in Beijing, China, the impact of view factors on intra-urban air temperature and thermal comfort was evaluated. Measurements were conducted along a selected path during hot summer days with clear skies and light winds by mobile traverses. The obtained results showed that SVF was positively correlated with air temperature during the day but negatively correlated with air temperature at night. BVF mainly played a warming role in both daytime and nighttime. Especially at night, BVF was the main geometric warming factor. TVF had a significant cooling effect during the day but did not have a negative effect at night due to reduced SVF. There was a strong point-to-point correlation between SVF and outdoor thermal comfort in the daytime. The mean differences in Mean Radiant Temperature and Physiologically Equivalent Temperature between shaded and unshaded sites were 12.0 °C and 6.8 °C, respectively, which suggested that providing effective shading is extremely important for improving outdoor daytime thermal comfort.

1. Introduction

* Corresponding author.

E-mail address: yanhai@zafu.edu.cn (H. Yan).

More than half of the world's population currently lives in urban areas, and this is expected to increase to two-thirds of the global population by the

middle of this century (United Nations, 2018). With the growing urban population and the enlarging urban scale, the original natural underlying surface of cities has been replaced by impervious surface, which has greatly altered the material and energy balance of the near surface in urban areas to form a unique urban climate (Oke, 1982). As the most significant feature of urban climate, urban heat island (UHI) has attracted considerable attention (Grimm et al., 2008; Deilami et al., 2018). Numerous studies have shown that the UHI effect exists in almost all cities around the world and that the UHI intensity gradually increases as cities expand (Levermore et al., 2018). The UHI effect has many adverse consequences on urban residents' living quality and urban ecological environment. On the one hand, UHIs affect air quality and increase the impact of extreme heat events, which exposes urban residents to higher health risks (Tan et al., 2010; Oleson et al., 2015). On the other hand, the high temperature caused by UHIs also increases power consumption in the hot season and greenhouse gases, which poses a serious threat to the ecological environment and sustainable development of cities (Santamouris et al., 2015). With global warming and a new round of urbanization, urban thermal environment problems are becoming more prominent and serious (Cao et al., 2018). Therefore, the study of the main influencing factors and regulatory mechanism of the urban thermal environment and the effective improvement of the urban thermal environment have been increasingly concerned by relevant scholars and managers (Lin et al., 2017).

The urban outdoor thermal environment largely depends on the local underlying surface characteristics, including two-dimensional (2D) landscape composition and three-dimensional (3D) geometric configuration (Oke, 1981; Yan et al., 2014a). At present, a large number of studies mainly focus on the impact of 2D landscape composition (buildings, green spaces, impervious surfaces, etc.) on the urban thermal environment (Yokobori and Ohta, 2009; Yan et al., 2014b; Zhou et al., 2017; Ziter et al., 2019; Aboelata and Sodoudi, 2020; Ouyang et al., 2020; Tepanosyan et al., 2021), while relatively little attention is paid to the impact of the 3D geometric configuration (Bärring et al., 1985; Eliasson, 1990; Unger, 2004; Unger, 2009; Li et al., 2020). Although the relative importance of 2D composition and 3D geometry on temperature has not been determined, some studies show that 3D geometric configuration may have a more significant impact on the urban thermal environment (Yin et al., 2018; Tian et al., 2019; Cao et al., 2021). The geometric configuration of the urban underlying surface, which is one of the key variables controlling the local distribution of near-surface energy, can block and guide air flow and affect the acceptance and loss of ground radiation. In urban climate research, the sky view factor (SVF), street height-to-width ratio (H/W) and street orientation are often used to quantify the urban geometry (Unger, 2004). Among them, SVF is the most widely used because it is accurate and easy to measure in complex urban environments.

SVF is defined as the fraction of the overlying hemisphere occupied by sky at a given point (Oke, 1981). It is a dimensionless quantity between 0 and 1, which represent complete obstruction and complete opening to the sky, respectively. During the daytime, in deep canyons with smaller SVF, less solar radiation reaches the ground, and the rise of the surface temperature and near-surface air temperature is slower (Bourbia and Boucheriba, 2010; Cheung and Jim, 2019; Zhang et al., 2019). The phenomenon of "urban cool island" observed in some studies is mainly due to a smaller SVF (Yan et al., 2014a; Hart and Sailor, 2009). For lower SVF, at nighttime, the heat dissipates slower, which leads to the UHI effect (Andreou and Axarli, 2012). However, some studies show that SVF has a limited influence on urban temperature, especially air temperature; thus, the impact of SVF should not be exaggerated (Upmanis and Chen, 1999; Krüger et al., 2011). Overall, the existing research shows that the relationship between SVF and urban temperature is rather contradictory (Unger, 2004). On the one hand, the SVF acquisition methods, study area size, sample number and observation time were different among these studies. On the other hand, the SVF of a given urban outdoor site is mainly determined by the structure of nearby buildings and tree canopy. However, the thermal properties of buildings and trees are quite different, and the proportion will inevitably influence the effects of SVF on the thermal environment (Wong

and Steve, 2010). Therefore, a single SVF cannot precisely quantify the urban geometry. Buildings and trees must also be considered.

In this context, we propose to use view factors (VFs), including sky, building and tree view factors (SVF, BVF, and TVF, respectively), to accurately quantify the 3D urban geometry. As three important parameters of the urban outdoor environment, SVF, BVF and TVF are defined as the geometric proportions of the visible number of the sky, buildings and trees at a given point, respectively (Johnson and Watson, 1984; Gong et al., 2018). The above parameters not only describe the ratio of the radiation received (or emitted) by urban streets to the total radiation received (or emitted) by the entire hemispheric radiation environment but also accurately describe the geometric characteristics of street canyons (Gong et al., 2018; Du et al., 2020), which provides the basis and possibility for an in-depth understanding of the relationship between urban geometry and the outdoor thermal environment. In this study, we investigate the spatial and temporal differences in air temperature at a local scale in Beijing to gain insights into its linkage to view factors. The specific objectives of this study are (1) to investigate how different VFs contribute to the variance in urban air temperature, (2) to analyze whether the relative importance of different VFs varies with time and local climate zones in explaining air temperature differences, and (3) to study the effect of SVF on outdoor thermal comfort to provide insights for urban planning and design.

2. Methodology

2.1. Study area

This study was carried out in Beijing, the capital of China with a population of 21.89 million. It has a warm temperate zone continental monsoon climate (Dwa under Koppen-Geiger climate classification), with a cold and dry winter and a hot and humid summer. Based on Beijing's climatological normals (1971–2000), January is the coldest month with an average temperature of -3.7°C , while July is the hottest month with an average temperature of 26.2°C . The wind is most often from the southeast in summer and the northwest in winter. The average annual rainfall is 571.9 mm, 74 % of which occur in summer.

Beijing Olympic Park and surrounding neighborhoods were selected as the study area, which is located at the northern end of the central axis of Beijing (Fig. 1). The study area has a rectangular shape of $3.1\text{ km} \times 1.7\text{ km}$, and the terrain in the area is flat; therefore, the influence of topography and altitude differences on microclimates can be ignored. The streets and buildings are mainly east-west and north-south orientations. To quantitatively analyze the relationship between outdoor thermal environment and VFs, a total of 121 uniformly distributed measurement points were selected in the study area. These points are limited to several square kilometers, which makes them all affected by a uniform meso-scale urban canopy layer climate. At the same time, these measuring points were separated by a certain distance; thus, they were also affected by different micro-scale urban environmental characteristics.

Similar to Wong et al. (2007), we can view this study area as a miniature "city" with diverse underlying surface compositions and configurations. According to the differences in the underlying surface type, the study area can be divided into the following three parts: the middle part is Olympic Park; the western part is a medium- and low-density residential area; and the eastern part is a high-density commercial and residential mixed building area (Table 1). The local climate zones (LCZ) scheme (Stewart and Oke, 2012), a standardized classification protocol for urban climate studies, has been applied to the classification of the study area. LCZ is defined by the surface properties, which are measurable and independent of time or space. Based on remote sensing images and field investigation, the study area was classified into three different LCZ types according to their surface properties, namely sky view factor, aspect ratio, mean building height, building surface fraction, impervious surface fraction and pervious surface fraction. The western part belongs to LCZ 5 (open mid-rise), the middle part belongs to LCZ B_E (scattered trees with paved roads), and the eastern part belongs to LCZ 4 (open high-rise). To explore whether the composition of

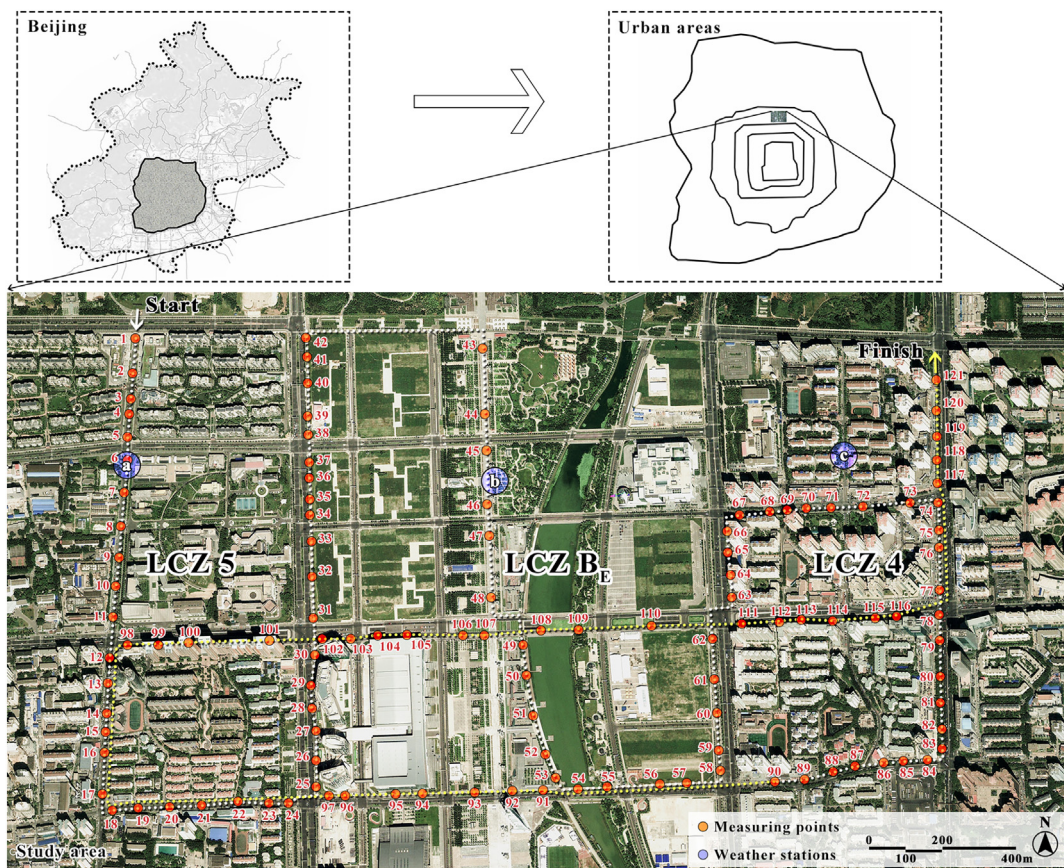


Fig. 1. Study area with measurement points and traverses. The dashed line indicates the measurement route. The points of the fisheye photos and air temperature measurements are specially marked with numbers. The fixed air temperature measurement stations (a-c) are also marked in the figure.

the underlying surface has an effect on air temperature, we selected 18 representative points in each of the three LCZs to further analyze the relationship between the air temperature and VFs in each zone. The selected measurement points are located on the north-south streets and are far away from the Olympic forest park, water bodies, crossroads and anthropogenic heat sources.

2.2. Microclimate parameter measurements

Mobile transects were used to conduct air temperature measurements along a fixed route with a distance of 13.5 km on 8 days between June and August 2013. Survey times for each day were early afternoon (14:00–15:00) and midnight (23:00–00:00). The previous studies show

Table 1
Landscape composition and landscape configuration characteristics of each zone.

LCZs	Selected points	LCZ schematics	Typical fisheye photos	SVF	BVF	TVF	PBS	PIS	PPS
LCZ 5	P1-P18			0.613 0.433–0.741	0.241 0.072–0.467	0.146 0.070–0.290	31.23	36.00	32.77
LCZ B _E	P31-P48			0.604 0.404–0.802	0.101 0.036–0.270	0.295 0.161–0.489	6.00	31.43	62.57
LCZ 4	P63-P66 P75-P83 P117-P121			0.388 0.224–0.589	0.200 0.005–0.506	0.412 0.056–0.642	26.27	44.53	29.2

Note: PBS, PIS, and PPS refer to the percent of building surface, the percent of impervious surface, and the percent of pervious surface to total plan area respectively.

that the range of intra-urban air temperature variability and the heat island is best expressed under favorable (calm and cloudless) weather conditions (Oke, 1981). The role of urban geometry has been examined during such conditions and these conditions also favor strong outgoing radiation. Avoidance of windy conditions also minimizes the influence that the air temperature of a measurement might have on surrounding sites through convection. Therefore, to minimize the influence of meteorological variables, air temperature data of three calm (the wind speed was required to be <2 m/s) and clear-sky conditions (the total sum of clouds observed was required to be equal to or less than 1 oktas) were chosen for further analysis in this study (Table 2). Cloud conditions, wind speed and direction were obtained from the weather station located in Beijing Olympic Park, operated by the China Meteorological Administration.

The measurements of air temperature were conducted by using a shielded temperature meter (TES-1365) mounted on the front of a bike at 1.5 m above the street surface. The accuracy of temperature sensor was $\pm 0.4^{\circ}\text{C}$ and the response time was <10 s at 1 m/s air flow (lower at higher wind speeds). The temperature sensor was configured to record data at an interval of 3 s and was calibrated prior to field measurements. As the sensor was not aspirated, the appropriate speed and the resulting relative wind speed are important to minimize lags in sensor response. Thus, the bicycle travels at a constant speed of 16 km/h without stopping. A wireless GPS logger (Holux M-241A) was used to synchronously record the longitude, latitude and time of movement, and the data collection interval of the trajectory recorder was 1 s. During the mobile observation period, three fixed weather stations were also arranged in the study area to record temperature changes in the different LCZs. The entire process of mobile observation took approximately 50 min; therefore, we corrected the air temperature of all the measurement points to the beginning time (14:00 and 23:00 respectively) according to the temperature change rate of the three fixed weather stations. For the traverses, the temperature at each site is represented by an average of three samples collected since arriving each measurement point over a 50 m transect in order to avoid the influence of small variations and sensor response lag.

2.3. Measurement and calculation of VFs

VFs were used to quantify the geometric structure of the urban canopy. For the determination of the VFs, fisheye photos at each measurement site were taken by a fisheye lens coupled with a digital camera. In Photoshop software, the fisheye photos were cropped to squares and exported to BMP format. And at the same time, the fisheye images were modified into black-and-white images to calculate SVF, in which the sky was processed into white while buildings and trees were processed into black. Similarly, we repeated the procedure for the other two VFs. Then, the processed images were put into RayMan 1.2, a free and widely used software developed by Matzarakis et al. (2010), for each VFs calculation. Detailed VF measurements and calculation processes are shown in Fig. 2.

2.4. Calculation of outdoor thermal comfort

The impact of SVF on outdoor thermal comfort was evaluated through the mean radiant temperature (MRT) and the physiologically equivalent temperature (PET). PET and MRT are essential indicators for objectively

evaluating the outdoor thermal environment. MRT is one of the meteorological parameters that can influence human energy balance and human thermal comfort. PET is a widely used thermal comfort index that is based on MRT, is reported in $^{\circ}\text{C}$, and expresses how people experience weather conditions by incorporating the radiative environment and personal characteristics, such as height, weight, age, clothing, and activity. The radiation and bioclimate model RayMan was utilized for the calculation of MRT and PET. By inputting the fisheye photographs and corresponding meteorological data in RayMan 1.2, the MRT and PET were calculated. In the parameter Settings of RayMan software, the standard conditions for anthropometric quantities were set with reference to the average height and weight of Chinese people, and were set as a 35-year-old healthy male, 170 cm in height and 70 kg in weight. For personal clothing and activity level, refer to ISO 7730 and ASHRAE Standard, wearing summer clothing (0.5 clo) and walking normally on level ground at 1.2 m/s (150 W/m², 2.6 met).

2.5. Data analysis

To reduce the accidental error of a one-day measurement, the mean values of three measuring days at different measuring times were taken as the temperature conditions of different measurement points. We first used linear regression analyses and a correlation analysis to examine the bivariate relationship between the indicators of the VF and air temperature. The Spearman's rank correlation coefficient (ρ) was used to evaluate the temporal and spatial relationship. We did not use Pearson correlation analysis because the indicators selected in this study did not follow a normal distribution. Furthermore, Spearman's ρ does not require a linear relationship between the statistical series of interest. In addition, the strength of association is quantified by correlating the ranks of observations, which has the additional advantage of being more robust to outliers. A linear regression analysis was also performed to investigate the effects of SVF on outdoor thermal comfort. All of the statistical analyses were performed in IBM SPSS Statistics 19.0 (IBM Corp., USA).

3. Results and analysis

3.1. Air temperature distribution and site geometry

The fisheye photos of selected representative measurement points and VF value variations along the measurement route are shown in Fig. 3a and d. In the study area, the SVF values varied from 0.095 to 0.849, the BVF values varied from 0.005 to 0.542, and the TVF values varied from 0 to 0.886, which implies that the study area exhibited extremely diverse urban geometry characteristics.

Fig. 3b shows the air temperature variations at different measuring points along the measurement route at 14:00. It can be seen from the figure that the air temperature fluctuated significantly at different measuring points, and the temperature variation trends on the three measuring days were similar. By comparing the average temperature, we found that the highest temperature occurred at measuring point 22, and the average air temperature reached 36.4°C . This measuring point was located in a wide east-west street, which was fully exposed to solar radiation during the day (Fig. 4a). Continuous heating by solar radiation led to the high air temperature of the impervious surface. The lowest air temperature occurred at measuring point 101, with an average temperature of 34.4°C . The point was also located on an east-west road and was shaded by high-rise buildings on the south side (Fig. 4b). This resulted in a relatively weak influence of solar radiation and a slow rise in air temperature during the day to thus form the so-called "urban cold island". Notably, the air temperature at point 88, which was located in the high-density commercial area, was also very low. This was mainly because the trees on both sides of the street provided good shading (Fig. 4c).

Fig. 3c shows the air temperature variations at different measuring points along the measurement route at 23:00. The air temperature at different measurement points on the three observation days shows similar changing patterns, and the variation in air temperature was more obvious at

Table 2
Weather conditions during the measurement period on selected days.

Date	Time	Air temperature ($^{\circ}\text{C}$)	Relative humidity (%)	Wind speed (m/s)	Wind direction	Cloud cover (oktas)
July 2, 2013	14:00	35.0	34	1.9	WNW	0.5
	23:00	26.0	70	0.9	WSW	0.2
July 3, 2013	14:00	36.1	37	0.8	NNE	0.3
	23:00	25.6	80	1.0	SW	0.0
July 5, 2013	14:00	35.3	33	0.8	WSW	0.5
	23:00	28.3	55	1.4	S	1.0

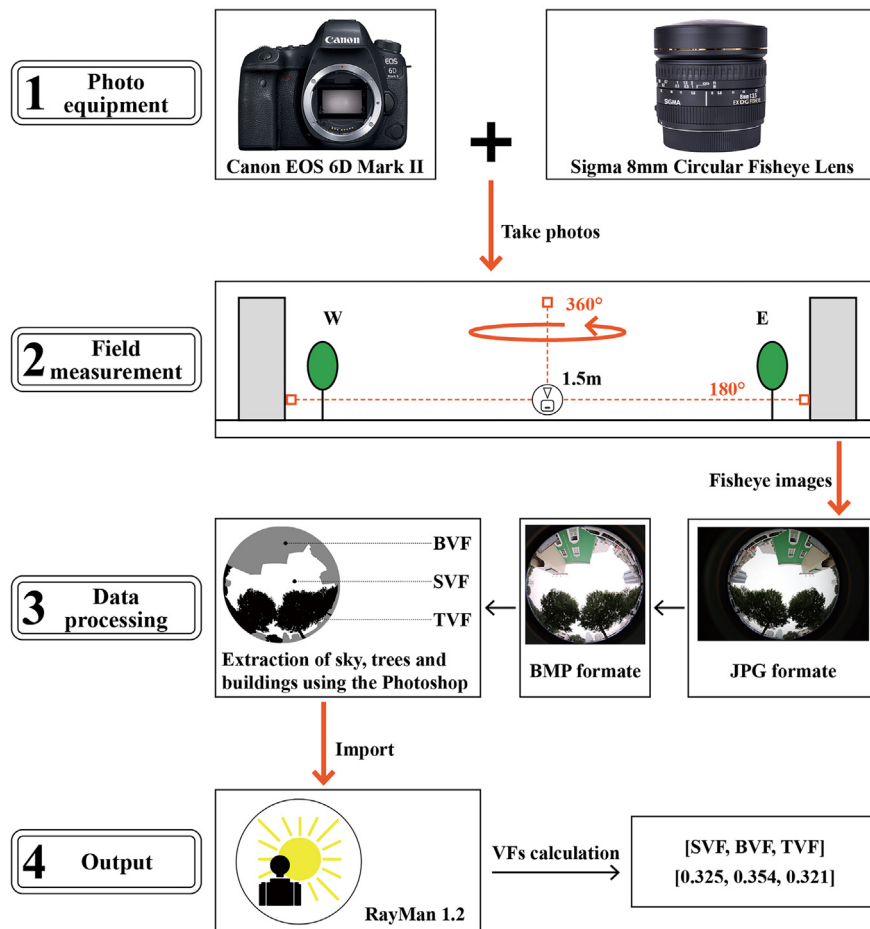


Fig. 2. Workflow chart of the VF calculation.

midnight than in the early afternoon. By comparing the average temperature, it was found that the lowest temperature occurred at measurement points 43 and 46, and the average air temperature was 29.7 °C. Both points showed high SVF and low BVF (Fig. 4d). Particularly, all of the low-temperature points were located in the park and exhibited an obvious “park cold island” effect, which indicates that the air temperature was also affected by the underlying surface composition to a certain extent. At this time, the highest temperature in the study area appeared at measuring points 78 and 79, and the average air temperature was 31.1 °C. Both measuring points showed high BVF and low TVF, which contributes to more heat absorption during the daytime and less heat dissipation at night and results in a higher air temperature (Fig. 4e and f).

3.2. Relationship between air temperature and VFs

As suggested in Fig. 3, the air temperature distribution shows a certain correlation with the urban surface geometry. We further explored the correlation by using simple linear regression analyses. As shown in Fig. 5, there was a weak positive correlation between SVF and air temperature at 14:00 ($R^2 = 0.040$, Fig. 5a). Similarly, BVF showed a positive effect on air temperature ($R^2 = 0.073$, Fig. 5b). In contrast, there was a significant negative relationship between air temperature and TVF ($R^2 = 0.146$, Fig. 5c). This suggests that during the day, the trees effectively blocked solar radiation through the shading effect, which led to a lower outdoor air temperature.

There was a strong negative relationship between the air temperature and SVF ($R^2 = 0.314$, Fig. 5d) and a strong positive relationship between the air temperature and BVF ($R^2 = 0.413$, Fig. 5e) at 23:00. However, there was almost no correlation between the air temperature and TVF ($R^2 = 0.005$,

Fig. 5f), which means that trees had little negative effect on the air temperature by lowering SVF at night.

Urban air temperature is known to be affected by the composition and geometry of the underlying surface. Therefore, we proposed the hypothesis that the relationship between air temperature and VFs differed in different urban zones. Then, the relationship between air temperature and VFs in the three LCZs was studied separately through a correlation analysis. The results of the statistical calculations are summarized in Table 3.

As shown in the table, the relationship between the SVF and air temperature in different LCZs was consistent at 14:00 and 23:00, and exhibited a positive correlation in the early afternoon and a negative correlation at midnight. The correlation coefficient between SVF and the air temperature was higher in the LCZs with a high homogeneity of underlying surface composition. However, the relationship between BVF and the temperature varied greatly at 14:00. For example, in LCZ 5 and LCZ 4, the BVF showed a weak negative correlation with the air temperature, which was mainly due to the cooling effect caused by the shading of some high-rise buildings. However, buildings without shading effects exhibited warming effects, such as those in LCZ Be. Similar to BVF, the correlation between TVF and the air temperature also varied greatly among different local zones in the early afternoon. In LCZ 5, due to the low view factor of trees and their location on the side, there was little effective shade; thus, the cooling effect of TVF was not obvious. In LCZ 4, although the visible factor of trees was high, the shading effect was partially offset due to the superposition of high-rise buildings; therefore, the relationship between TVF and the temperature was weak. Thus, during the day, the influence of BVF and TVF on the air temperature was limited by their number and location, that is, by the effective shade that they provided. At night, BVF was always the strongest warming factor, while TVF had no obvious warming effect.

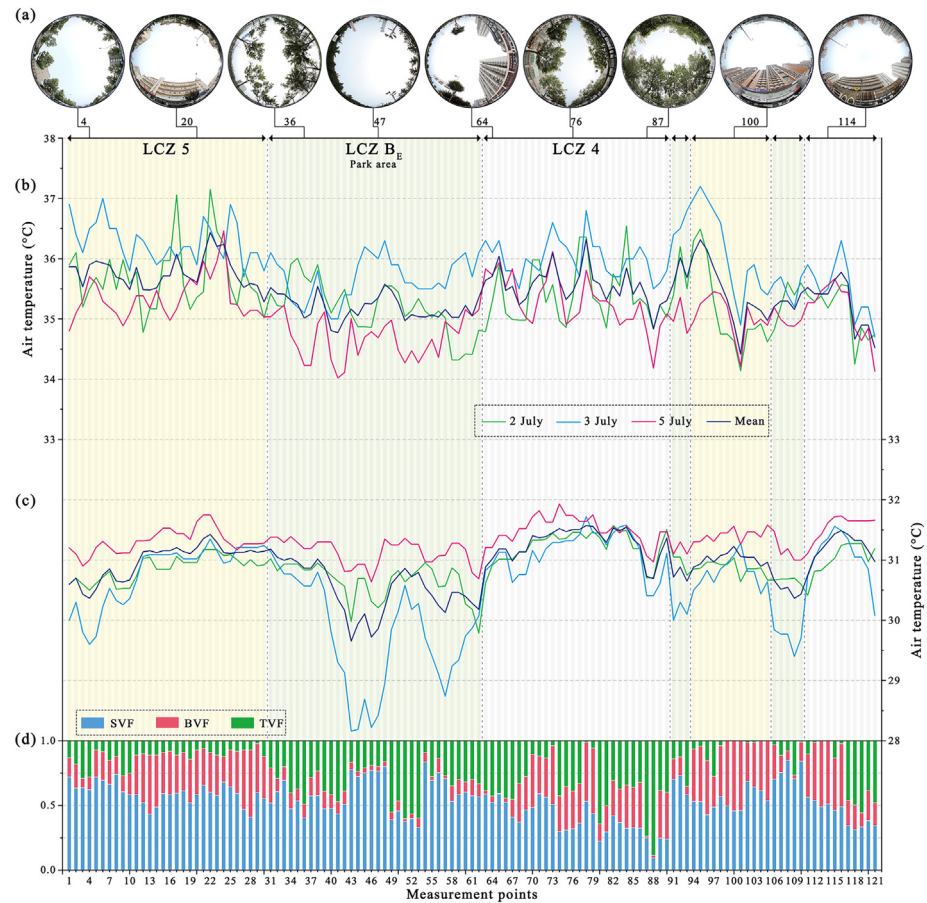


Fig. 3. The variation in air temperature and VFs along the measurement route. (a) selected typical fisheye lens photos, (b) air temperature profile at 14:00, (c) air temperature profile at 23:00, and (d) the variation in the VF values.

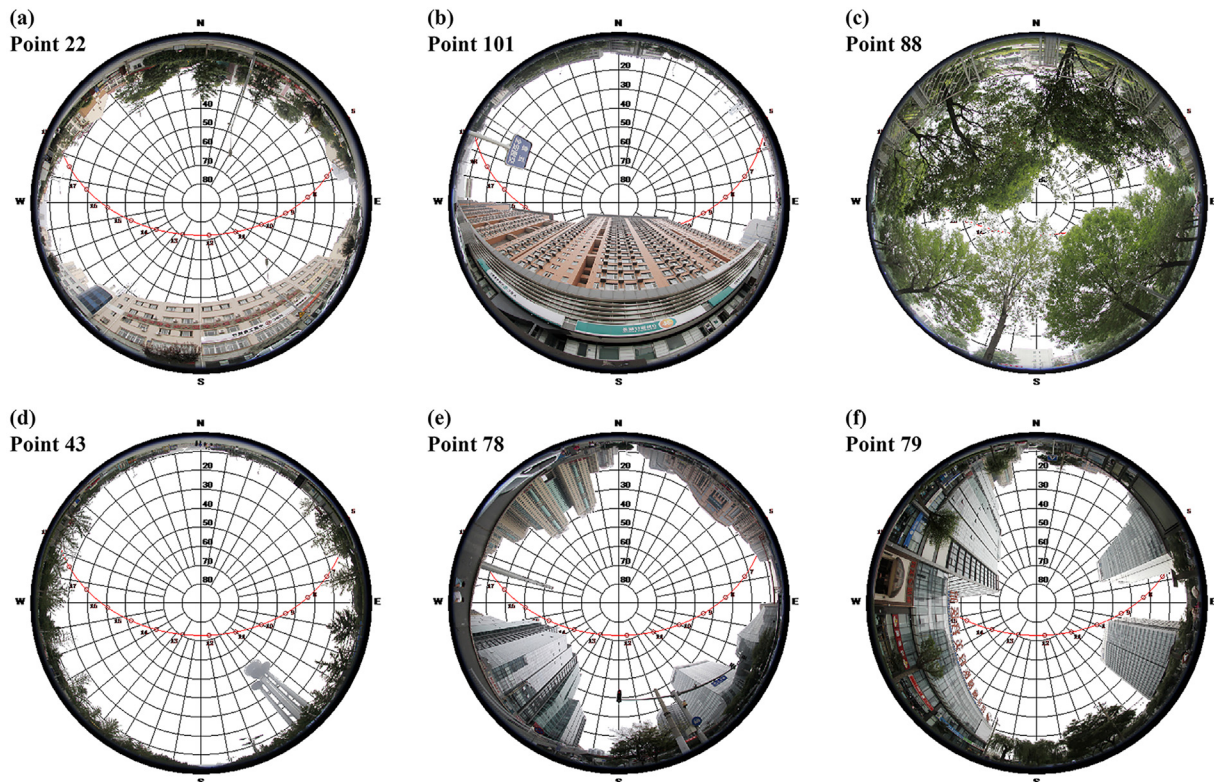


Fig. 4. Fisheye photos and sun trajectories of selected points for the July 3, 2013.

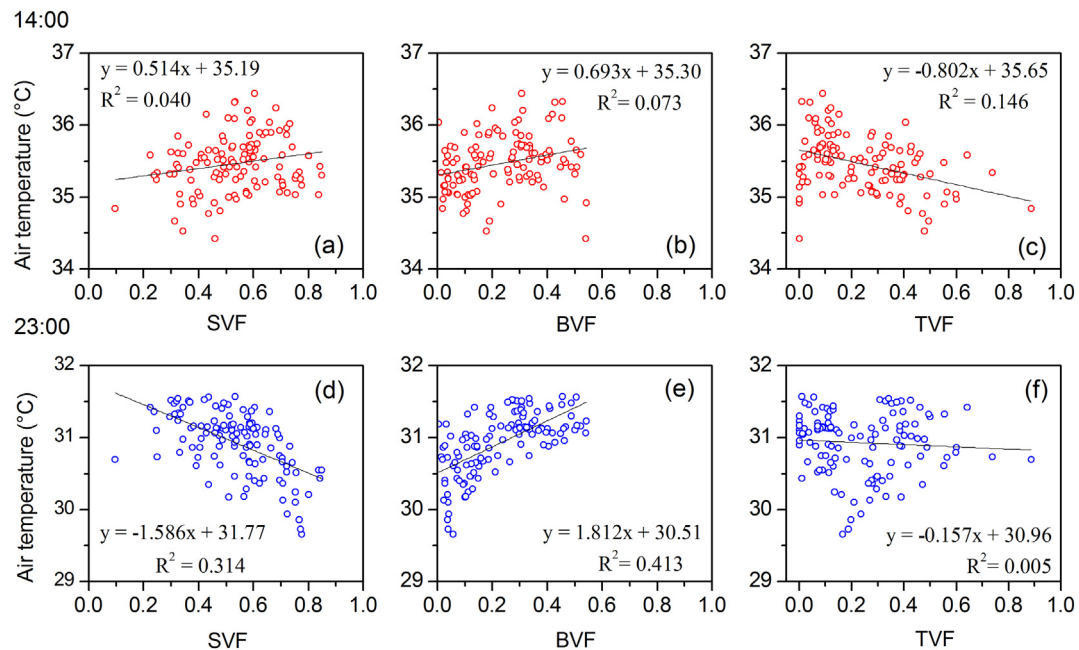


Fig. 5. Relationship between air temperature and VFs for all measuring points at 14:00 (a–c) and 23:00 (d–f).

3.3. Relationship between thermal comfort and SVF

The meteorological data and fisheye photos of each measurement point were imported into RayMan software to calculate the corresponding MRT and PET. Since the difference between trees and buildings cannot be distinguished during software analysis, only the influence of SVF on thermal comfort was discussed here. Fig. 6 shows the linear regression relationship between SVF and outdoor thermal comfort. As seen from the figure, in the early afternoon, both MRT and PET showed an increasing trend with the increase in SVF, which presents an extremely significant positive correlation

(Fig. 6a and b). Notably, both MRT and PET differentiate into two distinct and greatly different segments due to the influence of direct shading. The mean differences in MRT and PET between shaded and unshaded sites were 12.0 °C and 7.2 °C, respectively (Fig. 7). This result suggests that providing effective shading during the daytime is extremely important for improving urban outdoor thermal comfort. At midnight, SVF showed a significant negative correlation with MRT and PET (Fig. 6a and b). The determination coefficients of the regression equation were 0.951 and 0.842, respectively, which indicates that SVF could explain 95.1 % and 84.2 % of the MRT and PET changes, respectively.

Table 3

Spearman's rank correlation coefficients between the air temperatures and indicators of VFs for the three LCZs and for the entire measuring points.

Zones	14: 00			23: 00		
	SVF	BVF	TVF	SVF	BVF	TVF
All	0.184	0.323**	-0.335**	-0.552**	0.649**	-0.108
LCZ 5	0.601**	-0.248	-0.230	-0.637**	0.841**	-0.545*
LCZ B _E	0.490*	0.021	-0.612**	-0.511*	0.773**	0.387
LCZ 4	0.481*	-0.051	-0.389	-0.303	0.798**	-0.458
Spearman's ρ	-1	0	1			

Note: The correlations were quantified by means of Spearman's rank correlation coefficients (ρ). Colors represent the intensity and direction of the relationship—lower correlations are indicated in white, while orange and blue hues represent higher positive and negative correlation, respectively. Correlations significant at 0.05 and 0.01 level are marked with * and **, respectively.

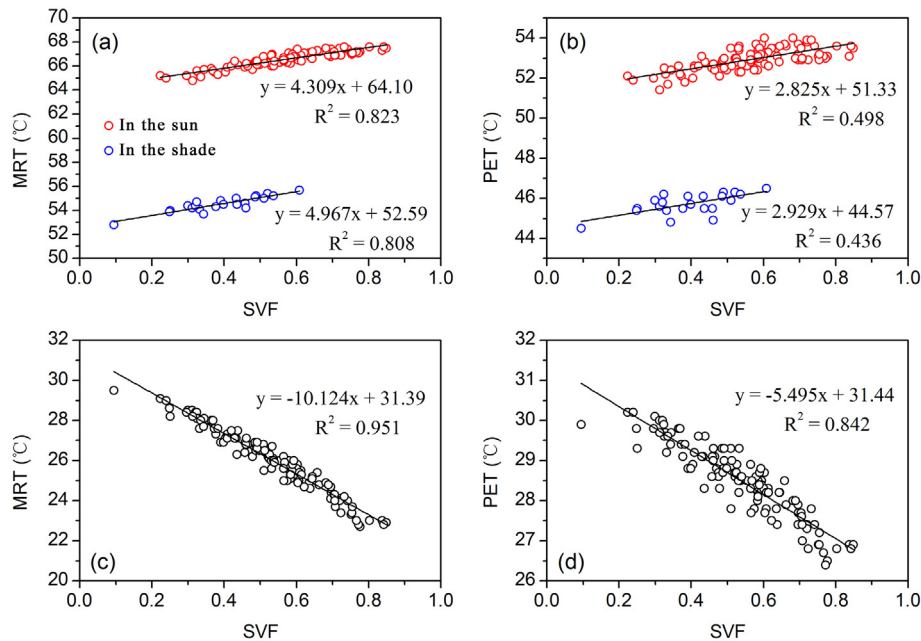


Fig. 6. Relationship between SVF and MRT as well as PET for all measuring points at 14:00 (a-b) and 23:00 (c-d).

4. Discussion

4.1. Heterogeneity in the neighborhood morphology and air temperature

By measuring the local outdoor microclimate in Beijing, we found that there were obvious differences in the air temperature even in small urban areas. In the early afternoon, the air temperature fluctuation at different measurement points was obvious, and the maximum average temperature difference was approximately 2 °C. This is mainly due to uneven heating during the day, which depends on exposure to direct solar radiation. Therefore, the air temperature of a measurement point is mainly affected by the geometric characteristics of its surrounding environment. Sites with higher air temperatures were usually located on open and unshaded streets, while those with lower air temperatures were usually surrounded by good shading from street trees or buildings. At midnight, the air temperature curve was relatively flat. Most areas with lower air temperatures were located in open parks, while areas with higher air temperatures were mainly located in high-density building areas. This result is in line with the research of Tian et al. (2019), which was carried out in residential neighborhoods in Beijing. The results suggest that during the nighttime, when solar radiation no longer exists and long wave radiation from the ground becomes the

main heat source, when the sky openness was higher, the air temperature was lower.

4.2. Influence of VFs on air temperature

4.2.1. Influence of SVF on air temperature

Urban geometry is an important factor that affects the urban microclimate (Oke, 1982). As an important urban geometric parameter, SVF and its relationship with urban temperature have been studied by a large number of scholars worldwide. Unfortunately, the conclusions are inconsistent and even contradictory (Unger, 2004). In this study, urban areas with different underlying surface compositions and structures were selected to investigate the impact of SVF on the urban air temperature. The results showed that the correlation between SVF and the air temperature was affected by several factors.

(1) Dependence on time

SVF was positively correlated with air temperature in the early afternoon and negatively correlated with air temperature at midnight, which is in accordance with other studies (Wong et al., 2007; Baghaeipoor and Nasrollahi, 2019). This is mainly due to the difference in the energy balance of the urban surface during the day and night. During the day, SVF regulates near-surface air temperature mainly by affecting direct solar radiation, while at night, SVF regulates air temperature mainly by affecting longwave radiation diffusion. This study also shows that the effect of SVF on air temperature was more significant at night, which is consistent with previous related studies (Svensson, 2004). Therefore, in the discussion on the relationship between SVF and air temperature, it is necessary to discuss the daytime and nighttime separately, and the use of an all-day average temperature can be misleading.

(2) Dependence on space (land cover composition)

Urban air temperature is influenced by the composition and structure of the underlying urban surface. The relationship between SVF and the air temperature is influenced by the composition of the underlying urban surface. This study found that the correlation between SVF and the air temperature was significantly stronger in LCZs with higher underlying surface homogeneity. A similar phenomenon was observed in Lisbon, Portugal (Vieira and Vasconcelos, 2003). By examining the relationship between SVF and the temperature for the entire city and 3 sample areas, it was

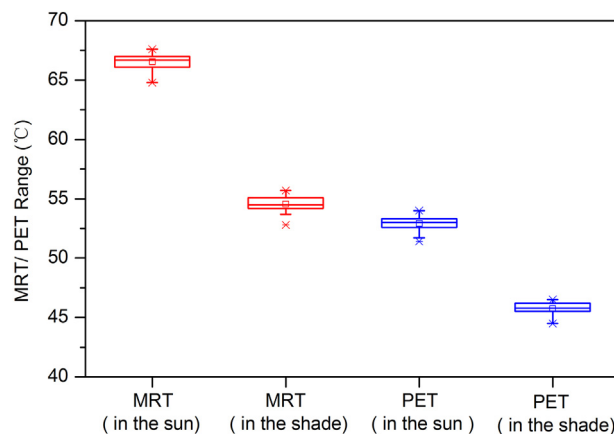


Fig. 7. Mean MRT and PET differences between measurements in the sun and in the shade at 14:00.

found that SVF had significant effect on surface temperature only in the urban center area. The main reason was that the underlying surface of the urban center area had a high homogeneity, i.e., high building coverage and low green coverage. Therefore, the influence of other site factors (e.g., land use and land cover, etc.) cannot be ignored when discussing the relationship between urban geometry and the urban thermal environment (Chow and Roth, 2006).

(3) The effect of BVF and TVF

The SVF value of any measurement point in an urban area is mainly determined by surrounding buildings and trees. This study found that BVF and TVF had opposite effects on air temperature. BVF mainly played a warming role, while TVF mainly played a cooling role. Therefore, the ratio of BVF and TVF will affect the correlation between SVF and the air temperature. Previous studies also found that the correlation between SVF and the air temperature was stronger in the season when trees shed their leaves (Unger, 2004). This is mainly because in winter, after the leaves fall, SVF is mainly determined by the architecture.

4.2.2. Influence of BVF on air temperature

In the early afternoon, BVF is weakly positively correlated with the air temperature. This is mainly due to the rapid heating of the building surface by solar radiation, which, in turn, heats the air and causes a higher air temperature. However, particularly, in some LCZs, BVF has a weak negative correlation with the temperature. This is mainly due to the shading effect of high-rise buildings, which makes the temperature rise slowly. This phenomenon has also been observed in previous studies (Chow and Roth, 2006; Tian et al., 2019; Deng and Wong, 2020). However, this cooling effect depends on the height and location of the building, which determine whether the building can provide effective shading. The opposing effects of buildings make the relationship between BVF and the air temperature ambiguous during the day. At midnight, BVF has a significant positive correlation with the air temperature and is the most important influencing factor of the air temperature during this time. This is partly because buildings receive more solar radiation and store more heat during the day, and the heat is gradually released at night (Ryu and Baik, 2012). On the other hand, due to the blockage of buildings, the diffusion of longwave radiation is slowed at night, as is the cooling progress (Unger, 2004). It is also possible that variations in wind caused by buildings will contribute to the observed air temperature differences (Chow and Roth, 2006). In addition, more buildings are associated with higher population densities with greater man-made heat release. As a result, more heat generation and slower heat diffusion lead to a higher nocturnal air temperature at high BVF sites (Tian et al., 2019).

4.2.3. Influence of TVF on air temperature

A large number of studies have confirmed that urban vegetation has an obvious cooling effect (Bowler et al., 2010). Increasing the amount of vegetation, especially trees, is one of the most effective strategies to improve the urban thermal environment (Aminipour et al., 2019). The results of this study show that TVF was negatively correlated with the air temperature and played a role in lowering air temperature. Especially in the early afternoon, trees had a significant cooling effect through shading. Therefore, TVF can also be regarded as an index of shading, and its effect has been confirmed by other studies (Hwang et al., 2015; Zhang et al., 2019). However, notably, the shading cooling effect depends on the species, coverage and spatial arrangement of trees (Morakinyo et al., 2018; Park et al., 2019; Abdi et al., 2020; Morakinyo et al., 2020). That is, a certain percentage of the impervious surface should be covered with trees to provide effective shade over roads or buildings to maximize the cooling effect (De Abreu-Harbich et al., 2015; Jamei and Rajagopalan, 2019; Lee et al., 2020). At night, TVF has a weak negative correlation with the air temperature. This is consistent with the findings of Wong and Steve (2010) that the canopy at night does not hinder the loss of longwave radiation from the ground, although it reduces SVF and thus does not have a negative impact on the urban thermal environment. Similarly, Cheung and Jim (2019) monitored the air temperature in 14 urban parks in Hong Kong, and showed that

there was no significant correlation between SVF and nighttime air temperature. The findings also suggest that trees did not slow nocturnal radiative cooling by reducing SVF in the same way that buildings reduced SVF.

4.3. Influence of SVF on thermal comfort

The urban outdoor thermal comfort level has an important impact on pedestrian comfort and safety, the travel mode of dwellers and the utilization of public space. MRT is an important variable of many thermal comfort indices and is directly related to solar radiation. Therefore, this study first discussed the influence of SVF on MRT. The results indicate that MRT, which was strongly affected by solar radiation, was more related to SVF than air temperature. The higher correlation between MRT and SVF has also been mentioned in previous studies (Krüger et al., 2011; Venhari et al., 2019). Specifically, SVF and MRT were significantly negatively correlated at night. However, in the daytime, there was a strong point-to-point correlation between SVF and MRT; that is, the correlation was affected by the presence or absence of direct shading by buildings or trees. The MRT value was directly related to the solar radiation at a given position, and the differences in MRT between shaded and unshaded measuring points with the same SVF could be as high as 11 °C. To a certain extent, this also indicates that SVF has certain limitations when quantifying urban outdoor thermal comfort during the day (Krüger et al., 2011).

The correlation between SVF and PET was nearly identical to that between SVF and MRT, which suggests the importance of solar radiation to human thermal comfort levels. Especially during the daytime, reducing radiation to the human body is more important than lowering the air temperature. This is because solar radiation contributes the most to the body's energy budget. Since SVF has opposite effects on human thermal comfort during the daytime and nighttime, the comprehensive benefits of SVF in different periods should be considered in practical applications. In this study, the differences between buildings and trees were not distinguished because the MRT and PET were obtained by software simulation. Therefore, it is necessary to explore the influence of BVF and TVF on outdoor thermal comfort in subsequent studies, which is of great value and significance to effectively guide urban planning and design.

4.4. Implication for urban planning

The results show that buildings and trees influenced urban outdoor air temperature by regulating SVF. The buildings, whether during the day or at night, mainly had warming effects. Although this study finds that buildings could reduce the near-ground air temperature by shading during the daytime, whether a building can provide effective shading depends on its height and location. Since most cities in China are large-scale, populous and have wide streets ($H/W < 0.5$), it is difficult to increase building height to provide effective shading for streets. Ali-Toudert and Mayer's (2006) research showed that in the subtropical latitudes, the thermal environment for wide streets ($H/W = 0.5$) is highly stressful and almost independent of the street orientation. Another important issue is to compare diurnal and nocturnal situations on the street by assessing the influence of urban geometry on thermal comfort during the day on one hand, and the cooling rate of the urban geometry at night on the other hand. Although some buildings can provide shading and a lower air temperature during the daytime, they will delay the diffusion of heat in urban areas at night, which increases the urban heat load and nighttime UHI intensity. Moreover, for cities such as Beijing with hot summers and cold winters, a high BVF also has a negative impact on the thermal environment in winter. Therefore, the shading strategy of deep canyons used by some low latitude tropical cities to alleviate the urban thermal environment is not suitable for temperate cities such as Beijing (Ali-Toudert et al., 2005; Emmanuel et al., 2007; Jamei et al., 2020). This shows that the latitude and climate characteristics must be taken into account when discussing the influence of urban geometry on the urban thermal environment.

In contrast, trees are more flexible and effective in regulating the urban outdoor thermal environment. During the day, trees can effectively regulate

the near-ground microclimate through shading, while at night, trees do not have a negative effect on the outdoor thermal environment. According to the research conducted by Du et al.'s (2020) in Beijing, VF determines the final characteristics of the sun duration in street canyons in which green vegetation and buildings block 41 % and 19 % of the typical sun duration, respectively. Sun et al.'s (2021) study in The City of Greater Bendigo, Australia also confirmed that tree shade is one of the most effective means of regulating urban SVF and thermal comfort. Thus, trees are more effective at blocking solar radiation during the daytime than buildings. Direct solar radiation strongly affects the urban outdoor microclimate and thermal comfort. Therefore, a reasonable selection of tree species and an increase in TVF can provide effective shading for the urban outdoor environment and adjust the near-ground radiation balance to thus effectively improve the urban outdoor thermal environment (Hwang et al., 2015; Morakinyo et al., 2017; Teshnehdel et al., 2020).

5. Conclusion

In this study, VFs were used to quantify the urban geometry, and then the influence of VFs on the urban outdoor thermal environment was investigated. The main findings of this study are as follows.

- 1) Urban geometry had an important effect on air temperature distribution at the local scale. In the early afternoon, low-temperature sites were usually located in areas with good shade from buildings or trees. At midnight, the cooler areas were mostly in park areas with open skies, while the warmer areas were mostly in the building areas of deep street canyons.
- 2) There was a positive correlation between SVF and air temperature in the early afternoon, while an inverse correlation was observed at midnight. The study also noted that the correlation between SVF and the air temperature largely depends on the composition of the underlying surface and the ratio between BVF and TVF.
- 3) BVF was weakly positively correlated with air temperature in the early afternoon. At midnight, BVF had a significant positive correlation with air temperature and was the most important influencing factor of air temperature during this time.
- 4) In the early afternoon, TVF was negatively correlated with air temperature, which suggests that trees can reduce the ambient air temperature through shading. At midnight, there was a weak negative correlation between TVF and the air temperature, which suggested that trees do not delay longwave radiation diffusion due to reduced sky openness and thus do not have a negative effect on nocturnal air temperature.
- 5) During the day, there was a strong point-to-point correlation between SVF and outdoor thermal comfort. The mean differences in MRT and PET between shaded and unshaded sites were 12.0 °C and 6.8 °C, respectively, which suggested that providing effective shading is extremely important for improving outdoor daytime thermal comfort.

This research was conducted in Beijing with a temperate climate, and the results may not be applicable to cities with other climate types. It is necessary to consider the geographical characteristics and seasonal characteristics of each city and adjust measures to local conditions.

CRediT authorship contribution statement

Hai Yan: Conceptualization, Writing – review & editing, Project administration. **Fan Wu:** Methodology, Software, Writing – original draft. **Xinge Nan:** Visualization, Conceptualization. **Qian Han:** Investigation, Software. **Feng Shao:** Supervision, Methodology. **Zhiyi Bao:** Writing – review & editing, Supervision.

Declaration of competing interest

The authors declare that they have no known competing financial interests or personal relationships that could have appeared to influence the work reported in this paper.

Acknowledgments

This research was funded by the Zhejiang Provincial Natural Science Foundation of China (Grant No. LGF21E080001) and the National Natural Science Foundation of China (Grant No. 51508515).

References

- Abdi, B., Hami, A., Zarehaghi, D., 2020. Impact of small-scale tree planting patterns on outdoor cooling and thermal comfort. *Sustain. Cities Soc.* 56, 102085. <https://doi.org/10.1016/j.scs.2020.102085>.
- Aboelata, A., Soudou, S., 2020. Evaluating the effect of trees on UHI mitigation and reduction of energy usage in different built up areas in Cairo. *Build. Environ.* 168, 106490. <https://doi.org/10.1016/j.buildenv.2019.106490>.
- Ali-Toudert, F., Mayer, H., 2006. Numerical study on the effects of aspect ratio and orientation of an urban street canyon on outdoor thermal comfort in hot and dry climate. *Build. Environ.* 41 (2), 94–108. <https://doi.org/10.1016/j.buildenv.2005.01.013>.
- Ali-Toudert, F., Djennane, M., Bensalem, R., Mayer, H., 2005. Outdoor thermal comfort in the old desert city of Beni-Isguen, Algeria. *Clim. Res.* 28 (3), 243–256. <https://doi.org/10.3354/cr028243>.
- Aminipour, M., Knudby, A.J., Krayenhoff, E.S., Zickfeld, K., Middel, A., 2019. Modelling the impact of increased street tree cover on mean radiant temperature across Vancouver's local climate zones. *Urban For. Urban Green.* 39, 9–17. <https://doi.org/10.1016/j.ufug.2019.01.016>.
- Andreou, E., Axarli, K., 2012. Investigation of urban canyon microclimate in traditional and contemporary environment. Experimental investigation and parametric analysis. *Renew. Energ.* 43, 354–363. <https://doi.org/10.1016/j.renene.2011.11.038>.
- Baghaipoor, G., Nasrollahi, N., 2019. The effect of sky view factor on air temperature in high-rise urban residential environments. *J. Daylighting* 6 (2), 42–51. <https://doi.org/10.15627/jd.2019.6>.
- Bärring, L., Mattsson, J.O., Lindqvist, S., 1985. Canyon geometry, street temperatures and urban heat island in Malmö, Sweden. *Int. J. Climatol.* 5 (4), 433–444. <https://doi.org/10.1002/joc.3370050410>.
- Bourbia, F., Boucheriba, F., 2010. Impact of street design on urban microclimate for semi arid climate (Constantine). *Renew. Energ.* 35 (2), 343–347. <https://doi.org/10.1016/j.renene.2009.07.017>.
- Bowler, D.E., Buyung-Ali, L., Knight, T.M., Pullin, A.S., 2010. Urban greening to cool towns and cities: a systematic review of the empirical evidence. *Landscape. Urban Plan.* 97 (3), 147–155. <https://doi.org/10.1016/j.landurbplan.2010.05.006>.
- Cao, Q., Yu, D., Georgescu, M., Wu, J., Wang, W., 2018. Impacts of future urban expansion on summer climate and heat-related human health in eastern China. *Environ. Int.* 112, 134–146. <https://doi.org/10.1016/j.envint.2017.12.027>.
- Cao, Q., Luan, Q., Liu, Y., Wang, R., 2021. The effects of 2D and 3D building morphology on urban environments: a multi-scale analysis in the Beijing metropolitan region. *Build. Environ.* 192, 107635. <https://doi.org/10.1016/j.buildenv.2021.107635>.
- Cheung, P.K., Jim, C.Y., 2019. Effects of urban and landscape elements on air temperature in a high-density subtropical city. *Build. Environ.* 164, 106362. <https://doi.org/10.1016/j.buildenv.2019.106362>.
- Chow, W.T., Roth, M., 2006. Temporal dynamics of the urban heat island of Singapore. *Int. J. Climatol.* 26 (15), 2243–2260. <https://doi.org/10.1002/joc.1364>.
- De Abreu-Harbich, L.V., Labaki, L.C., Matzarakis, A., 2015. Effect of tree planting design and tree species on human thermal comfort in the tropics. *Landscape. Urban Plan.* 138, 99–109. <https://doi.org/10.1016/j.landurbplan.2015.02.008>.
- Deilami, K., Kamruzzaman, M., Liu, Y., 2018. Urban heat island effect: a systematic review of spatio-temporal factors, data, methods, and mitigation measures. *Int. J. Appl. Earth Obs. Geoinf.* 67, 30–42. <https://doi.org/10.1016/j.jag.2017.12.009>.
- Deng, J.Y., Wong, N.H., 2020. Impact of urban canyon geometries on outdoor thermal comfort in central business districts. *Sustain. Cities Soc.* 53, 101966. <https://doi.org/10.1016/j.scs.2019.101966>.
- Du, K., Ning, J., Yan, L., 2020. How long is the sun duration in a street canyon?—Analysis of the view factors of street canyons. *Build. Environ.* 172, 106680. <https://doi.org/10.1016/j.buildenv.2020.106680>.
- Eliasson, I., 1990. Urban geometry, surface temperature and air temperature. *Energy Build.* 15 (1–2), 141–145. [https://doi.org/10.1016/0378-7789\(90\)90125-3](https://doi.org/10.1016/0378-7789(90)90125-3).
- Emmanuel, R., Rosenlund, H., Johansson, E., 2007. Urban shading—a design option for the tropics? A study in Colombo, Sri Lanka. *Int. J. Climatol.* 27 (14), 1995–2004. <https://doi.org/10.1002/joc.1609>.
- Gong, F.Y., Zeng, Z.C., Zhang, F., Li, X., Ng, E., Norford, L.K., 2018. Mapping sky, tree, and building view factors of street canyons in a high-density urban environment. *Build. Environ.* 134, 155–167. <https://doi.org/10.1016/j.buildenv.2018.02.042>.
- Grimm, N.B., Faeth, S.H., Golubiewski, N.E., Redman, C.L., Wu, J., Bai, X., et al., 2008. Global change and the ecology of cities. *Science* 319 (5864), 756–760. <https://doi.org/10.1126/science.1150195>.
- Hart, M.A., Sailor, D.J., 2009. Quantifying the influence of land-use and surface characteristics on spatial variability in the urban heat island. *Theor. Appl. Climatol.* 95 (3), 397–406. <https://doi.org/10.1007/s00704-008-0017-5>.
- Hwang, Y.H., Lum, Q.J.G., Chan, Y.K.D., 2015. Micro-scale thermal performance of tropical urban parks in Singapore. *Build. Environ.* 94, 467–476. <https://doi.org/10.1016/j.buildenv.2015.10.003>.
- Jamei, E., Rajagopalan, P., 2019. Effect of street design on pedestrian thermal comfort. *Archit. Sci. Rev.* 62 (2), 92–111. <https://doi.org/10.1080/00038628.2018.1537236>.
- Jamei, E., Ossen, D.R., Seyedmahmoudian, M., Sandanayake, M., Stojcevski, A., Horan, B., 2020. Urban design parameters for heat mitigation in tropics. *Renew. Sust. Energ. Rev.* 134, 110362. <https://doi.org/10.1016/j.rser.2020.110362>.

- Johnson, G.T., Watson, I.D., 1984. The determination of view-factors in urban canyons. *J. Appl. Meteorol. Climatol.* 23 (2), 329–335. [https://doi.org/10.1175/1520-0450\(1984\)023<0329:TDOVFI>2.0.CO;2](https://doi.org/10.1175/1520-0450(1984)023<0329:TDOVFI>2.0.CO;2).
- Krüger, E.L., Minella, F.O., Rasia, F., 2011. Impact of urban geometry on outdoor thermal comfort and air quality from field measurements in Curitiba, Brazil. *Build. Environ.* 46 (3), 621–634. <https://doi.org/10.1016/j.buildenv.2010.09.006>.
- Lee, H., Mayer, H., Kuttler, W., 2020. Impact of the spacing between tree crowns on the mitigation of daytime heat stress for pedestrians inside EW urban street canyons under Central European conditions. *Urban for. Urban Gree.* 48, 126558. <https://doi.org/10.1016/j.ufug.2019.126558>.
- Levermore, G., Parkinson, J., Lee, K., Laycock, P., Lindley, S., 2018. The increasing trend of the urban heat island intensity. *Urban Clim.* 24, 360–368. <https://doi.org/10.1016/j.ulclim.2017.02.004>.
- Li, G., Ren, Z., Zhan, C., 2020. Sky view factor-based correlation of landscape morphology and the thermal environment of street canyons: a case study of Harbin, China. *Build. Environ.* 169, 106587. <https://doi.org/10.1016/j.buildenv.2019.106587>.
- Lin, P., Gou, Z., Lau, S.S.Y., Qin, H., 2017. The impact of urban design descriptors on outdoor thermal environment: a literature review. *Energies* 10 (12), 2151. <https://doi.org/10.3390/en10122151>.
- Matzarakis, A., Rutz, F., Mayer, H., 2010. Modelling radiation fluxes in simple and complex environments: basics of the RayMan model. *Int. J. Biometeorol.* 54 (2), 131–139. <https://doi.org/10.1007/s00484-009-0261-0>.
- Morakinyo, T.E., Kong, L., Lau, K.K.L., Yuan, C., Ng, E., 2017. A study on the impact of shadow-cast and tree species on in-canyon and neighborhood's thermal comfort. *Build. Environ.* 115, 1–17. <https://doi.org/10.1016/j.buildenv.2017.01.005>.
- Morakinyo, T.E., Lau, K.K.L., Ren, C., Ng, E., 2018. Performance of Hong Kong's common trees species for outdoor temperature regulation, thermal comfort and energy saving. *Build. Environ.* 137, 157–170. <https://doi.org/10.1016/j.buildenv.2018.04.012>.
- Morakinyo, T.E., Ouyang, W., Lau, K.K.L., Ren, C., Ng, E., 2020. Right tree, right place (urban canyon): tree species selection approach for optimum urban heat mitigation-development and evaluation. *Sci. Total Environ.* 719, 137461. <https://doi.org/10.1016/j.scitotenv.2020.137461>.
- Oke, T.R., 1981. Canyon geometry and the nocturnal urban heat island: comparison of scale model and field observations. *Int. J. Climatol.* 1 (3), 237–254. <https://doi.org/10.1002/joc.3370010304>.
- Oke, T.R., 1982. The energetic basis of the urban heat island. *Q. J. R. Meteorol. Soc.* 108 (455), 1–24. <https://doi.org/10.1002/qj.49710845502>.
- Oleson, K.W., Monaghan, A., Wilhelm, O., Barlage, M., Brunsell, N., Feddema, J., et al., 2015. Interactions between urbanization, heat stress, and climate change. *Clim. Chang.* 129 (3), 525–541. <https://doi.org/10.1007/s10584-013-0936-8>.
- Ouyang, W., Morakinyo, T.E., Ren, C., Ng, E., 2020. The cooling efficiency of variable greenery coverage ratios in different urban densities: a study in a subtropical climate. *Build. Environ.* 174, 106772. <https://doi.org/10.1016/j.buildenv.2020.106772>.
- Park, C.Y., Lee, D.K., Krayenhoff, E.S., Heo, H.K., Hyun, J.H., Oh, K., et al., 2019. Variations in pedestrian mean radiant temperature based on the spacing and size of street trees. *Sustain. Cities Soc.* 48, 101521. <https://doi.org/10.1016/j.scs.2019.101521>.
- Ryu, Y.H., Baik, J.J., 2012. Quantitative analysis of factors contributing to urban heat island intensity. *J. Appl. Meteorol. Climatol.* 51 (5), 842–854. <https://doi.org/10.1175/JAMC-D-11-098.1>.
- Santamouris, M., Cartalis, C., Synnefa, A., Kolokotsa, D., 2015. On the impact of urban heat island and global warming on the power demand and electricity consumption of buildings—a review. *Energy Build.* 98, 119–124. <https://doi.org/10.1016/j.enbuild.2014.09.052>.
- Stewart, I.D., Oke, T.R., 2012. Local climate zones for urban temperature studies. *Bull. Am. Meteorol. Soc.* 93 (12), 1879–1900. <https://doi.org/10.1175/BAMS-D-11-00019.1>.
- Sun, Q., Macleod, T., Both, A., Hurley, J., Butt, A., Amati, M., 2021. A human-centred assessment framework to prioritise heat mitigation efforts for active travel at city scale. *Sci. Total Environ.* 763, 143033. <https://doi.org/10.1016/j.scitotenv.2020.143033>.
- Svensson, M.K., 2004. Sky view factor analysis—implications for urban air temperature differences. *Meteorol. Appl.* 11 (3), 201–211. <https://doi.org/10.1017/S1350482704001288>.
- Tan, J., Zheng, Y., Tang, X., Guo, C., Li, L., Song, G., et al., 2010. The urban heat island and its impact on heat waves and human health in Shanghai. *Int. J. Biometeorol.* 54 (1), 75–84. <https://doi.org/10.1007/s00484-009-0256-x>.
- Tepanosyan, G., Muradyan, V., Hovsepyan, A., Pinigin, G., Medvedev, A., Asmaryan, S., 2021. Studying spatial-temporal changes and relationship of land cover and surface Urban Heat Island derived through remote sensing in Yerevan, Armenia. *Build. Environ.* 187, 107390. <https://doi.org/10.1016/j.buildenv.2020.107390>.
- Teshnehzed, S., Akbari, H., Di Giuseppe, E., Brown, R.D., 2020. Effect of tree cover and tree species on microclimate and pedestrian comfort in a residential district in Iran. *Build. Environ.* 178, 106899. <https://doi.org/10.1016/j.buildenv.2020.106899>.
- Tian, Y., Zhou, W., Qian, Y., Zheng, Z., Yan, J., 2019. The effect of urban 2D and 3D morphology on air temperature in residential neighborhoods. *Landscape Ecol.* 34 (5), 1161–1178. <https://doi.org/10.1007/s10980-019-00834-7>.
- Unger, J., 2004. Intra-urban relationship between surface geometry and urban heat island: review and new approach. *Clim. Res.* 27 (3), 253–264. <https://doi.org/10.3354/cr027253>.
- Unger, J., 2009. Connection between urban heat island and sky view factor approximated by a software tool on a 3D urban database. *Int. J. Environ. Pollut.* 36 (1–3), 59–80. <https://doi.org/10.1504/IJEP.2009.021817>.
- United Nations, 2018. World Urbanization Prospects: The 2018 Revision. URL, <https://population.un.org/wup/>. Accessed 10-10-2021.
- Upmanis, H., Chen, D., 1999. Influence of geographical factors and meteorological variables on nocturnal urban-park temperature differences—a case study of summer 1995 in Göteborg, Sweden. *Clim. Res.* 13 (2), 125–139. <https://doi.org/10.3354/cr013125>.
- Venharai, A.A., Tenpierik, M., Taleghani, M., 2019. The role of sky view factor and urban street greenery in human thermal comfort and heat stress in a desert climate. *J. Arid Environ.* 166, 68–76. <https://doi.org/10.1016/j.jaridenv.2019.04.009>.
- Vieira, H., Vasconcelos, J., 2003. Urban morphology characterisation to include in a GIS for climatic purposes in Lisbon. Discussion of two different methods. *Proc 5th Int Conf on Urban Climate.* 2, pp. 417–420.
- Wong, N.H., Steve, K.J., 2010. Air temperature distribution and the influence of sky view factor in a green Singapore estate. *J. Urban Plann. Dev.* 136 (3), 261–272. [https://doi.org/10.1061/\(ASCE\)UP.1943-5444.0000014](https://doi.org/10.1061/(ASCE)UP.1943-5444.0000014).
- Wong, N.H., Jusuf, S.K., La Win, A.A., Thu, H.K., Negara, T.S., Xuchao, W., 2007. Environmental study of the impact of greenery in an institutional campus in the tropics. *Build. Environ.* 42 (8), 2949–2970. <https://doi.org/10.1016/j.buildenv.2006.06.004>.
- Yan, H., Fan, S., Guo, C., Wu, F., Zhang, N., Dong, L., 2014. Assessing the effects of landscape design parameters on intra-urban air temperature variability: the case of Beijing, China. *Build. Environ.* 76, 44–53. <https://doi.org/10.1016/j.buildenv.2014.03.007>.
- Yan, H., Fan, S., Guo, C., Hu, J., Dong, L., 2014b. Quantifying the impact of land cover composition on intra-urban air temperature variations at a mid-latitude city. *PLoS One* 9 (7), e102124. <https://doi.org/10.1371/journal.pone.0102124>.
- Yin, C., Yuan, M., Lu, Y., Huang, Y., Liu, Y., 2018. Effects of urban form on the urban heat island effect based on spatial regression model. *Sci. Total Environ.* 634, 696–704. <https://doi.org/10.1016/j.scitotenv.2018.03.350>.
- Yokobori, T., Ohta, S., 2009. Effect of land cover on air temperatures involved in the development of an intra-urban heat island. *Clim. Res.* 39 (1), 61–73. <https://doi.org/10.3354/cr00800>.
- Zhang, J., Gou, Z., Lu, Y., Lin, P., 2019. The impact of sky view factor on thermal environments in urban parks in a subtropical coastal city of Australia. *Urban For. Urban Green.* 44, 126422. <https://doi.org/10.1016/j.ufug.2019.126422>.
- Zhou, W., Wang, J., Cadena, M.L., 2017. Effects of the spatial configuration of trees on urban heat mitigation: a comparative study. *Remote Sens. Environ.* 195, 1–12. <https://doi.org/10.1016/j.rse.2017.03.043>.
- Ziter, C.D., Pedersen, E.J., Kucharik, C.J., Turner, M.G., 2019. Scale-dependent interactions between tree canopy cover and impervious surfaces reduce daytime urban heat during summer. *Proc. Natl. Acad. Sci.* 116 (15), 7575–7580. <https://doi.org/10.1073/pnas.1817561116>.